

# Enlargement in *Chara* Studied with a Turgor Clamp<sup>1</sup>

## Growth Rate Is Not Determined by Turgor

Guo Li Zhu and John S. Boyer\*

College of Marine Studies and College of Agriculture, University of Delaware, Lewes, Delaware 19958

### ABSTRACT

A new method, the turgor clamp, was developed to test the effects of turgor on cell enlargement. The method used a pressure probe to remove or inject cell solution and change the turgor without altering the external environment of the cell walls. After the injections, the cells were permanently at the new turgor and required no further manipulation. Internode cells of *Chara corallina* grew rapidly with the pressure probe in place when growth was monitored with a position transducer. Growth-induced water potentials were negligible and turgor effects could be studied simply. As turgor was decreased, there was a threshold below which no growth occurred, and only reversible elastic/viscoelastic changes could be seen. Above the threshold, growth was superimposed on the elastic/viscoelastic effects. The rate of growth did not depend on turgor. Instead, the rate was highly dependent on energy metabolism as shown by inhibitors that rapidly abolished growth without changing the turgor. However, turgors could be driven above the maximum normally attainable by the cell, and these caused growth to respond as though plastic deformation of the walls was beginning, but the deformation caused wounding. Growth was inhibited when turgor was changed with osmotica but not inhibited when similar changes were made with the turgor clamp. It was concluded that osmotica caused side effects that could be mistaken for turgor effects. The presence of a turgor threshold indicates that turgor was required for growth. However, because turgor did not control the rate, it appears incorrect to consider the rate to be determined by a turgor-dependent plastic deformation of wall polymers. Instead, above the turgor threshold, the rapid response to energy inhibitors suggests a control by metabolic reactions causing synthesis and/or extension of wall polymers.

It is well accepted that  $\psi_p^2$  is involved in cell enlargement. The evidence is based mostly on varying the  $\psi_p$  with osmotica or soil water deficits and observing changes in growth rates. These treatments also alter the solute and/or pressure environment of the cell walls (2, 11, 40), which raises the possi-

bility that side effects on wall metabolism could complicate the conclusions. Some studies avoided the complications by applying unidirectional tensions to cells or isolated cell walls (9, 10, 20, 25, 31, 35, 42), but the tensions may not have completely simulated  $\psi_p$ , which is multidimensional (31, 40).

After the elegant investigations of isolated cell walls by Preston and coworkers (33, 35), it was proposed that  $\psi_p$  causes an irreversible deformation of the wall to a larger size by a time-dependent plastic yielding resembling a steady creep (27, 28, 33). In some studies, creep appeared proportional to the  $\psi_p$  above a minimum termed the yield threshold (8, 35). Lockhart (27, 28) formalized these concepts in an equation of the form:

$$G = M(\psi_p - Y) \quad (1)$$

where  $G$  is the relative growth rate ( $\text{m}^3 \cdot \text{m}^{-3} \cdot \text{s}^{-1}$  or  $\text{s}^{-1}$ ),  $\psi_p$  is the turgor (MPa),  $Y$  is the yield threshold turgor (MPa), and  $M$  is the wall extensibility ( $\text{m}^3 \cdot \text{m}^{-3} \cdot \text{s}^{-1} \cdot \text{MPa}^{-1}$  or  $\text{s}^{-1} \cdot \text{MPa}^{-1}$ ).

Equation 1 has been extensively used (2, 40) but often without distinguishing growth from elastic changes. In a central study in *Nitella* (18), the  $\psi_p$  was changed with osmotica, but growth often did not change and elastic changes were not reported. In *Phycomyces*, increasing the  $\psi_p$  often caused only transitory changes in enlargement (32). Shackel et al. (37) found little relationship between  $\psi_p$  and growth in grape leaves. However, elastic responses to  $\psi_p$  were observed in mature *Nitella* cells (23). These differences between theory and observation indicate the importance of distinguishing between elastic and growth responses and call into question the exact role of  $\psi_p$ .

In the present work, we reexamined the role of  $\psi_p$  in cell enlargement by developing a method to change and maintain the  $\psi_p$  at any level without altering the external environment. With the method,  $\psi_p$  in large cells was changed by injecting solution previously collected from other cells growing in the same medium. Also, by monitoring the length of the cells, we could distinguish between elastic effects and growth.

<sup>1</sup> This work was supported by grants from the Department of Energy (DE-FG02-87ER13776) and E.I. DuPont Co.

<sup>2</sup> Abbreviations:  $\psi_p$ , turgor (MPa);  $Y$ , yield threshold turgor (MPa);  $M$ , extensibility ( $\text{m}^3 \cdot \text{m}^{-3} \cdot \text{s}^{-1} \cdot \text{MPa}^{-1}$  or  $\text{s}^{-1} \cdot \text{MPa}^{-1}$ );  $\psi_w$ , water potential of a cell (MPa);  $\psi_s$ , osmotic potential of a cell (MPa);  $\psi_o$ , water potential of nutrient solution (MPa);  $\psi_{pf}$ , final turgor;  $\psi_{pi}$ , initial turgor;  $\epsilon$ , volumetric elastic modulus of a cell (MPa);  $V$ , volume of a cell before injection ( $\text{m}^3$ );  $V_A$ , volume of cell solution injected into a cell

to change turgor;  $n_{sA}$ , mol of solute in volume  $V_A$ ;  $V_B$ , volume of cell solution injected into a cell to maintain turgor;  $n_{sB}$ , mol of solute in volume  $V_B$ ;  $V_T$ , total volume of injected solution ( $= V_A + V_B$ );  $L_p$ , hydraulic conductivity of cell membranes ( $\text{m} \cdot \text{s}^{-1} \cdot \text{MPa}^{-1}$ );  $t_{1/2}$ , half-time for turgor relaxation(s);  $A$ , surface area of cell ( $\text{m}^2$ );  $R$ , gas constant ( $\text{m}^3 \cdot \text{MPa} \cdot \text{mol}^{-1} \cdot \text{K}^{-1}$ );  $T$ , absolute temperature (K); FCCP, carbonyl cyanide *p*-trifluoromethoxyphenylhydrazone.

## THEORY

The technique is termed a turgor clamp because it (a) changes and (b) maintains (clamps) the  $\psi_p$  of cells by adding or removing cell solution from the vacuole using a pressure probe (Fig. 1). Assume that the cell is essentially in equilibrium with the water potential of the nutrient solution ( $\psi_o$ ):

$$\psi_s + \psi_p = \psi_w = \psi_o \quad (2)$$

where  $\psi_s$  is the osmotic potential and  $\psi_w$  is the water potential of the cell. The following theory is based on concepts given by Steudle (38).

### Changing the $\psi_p$

Cell solution is injected into the vacuole to increase  $\psi_p$  by an amount  $\Delta\psi_p = (\psi_{pf} - \psi_{pi})$ , where the subscripts *f* and *i* are the final and initial  $\psi_p$ , respectively (A in Fig. 1). The  $\Delta\psi_p$  adds a small volume  $V_A$  of water to the cell. In general,  $\Delta\psi_p = \epsilon(V_A/V)$ , where  $\epsilon$  is the bulk (volumetric) elastic modulus and  $V$  is the initial volume of the cell. Accordingly:

$$V_A = \frac{\Delta\psi_p V}{\epsilon} \quad (3)$$

Because the injected solution  $V_A$  has the same  $\psi_s$  as the cell,  $\psi_s$  is unchanged. However, the injection adds  $n_{sA}$  mol of solute to the cell. In general,  $V\psi_s = -RTn_s$  for dilute solutions, where  $R$  is the gas constant,  $T$  is the temperature in Kelvin, and  $n_s$  is the number of mol of solute. Accordingly, the amount of solute added is:

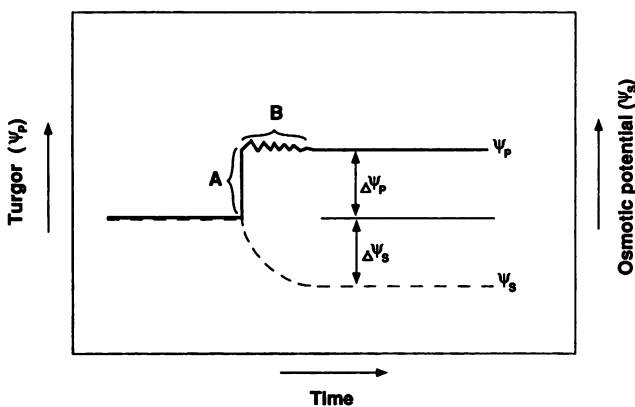


**Figure 1.** Schematic diagram of the turgor clamp. A, Changing the  $\psi_p$ . After the  $\psi_{pi}$  is obtained in a cell, an injection of cell solution of volume  $V_A$  will induce a sudden increase in  $\psi_p$  by  $\Delta\psi_p$  but no change in  $\psi_s$ . Without any further manipulation, the  $\psi_p$  would relax toward the original level. B, Maintaining the  $\psi_p$ . To prevent the  $\psi_p$  from relaxing, repeated small injections are given. Because the cell is not in equilibrium with the surrounding water, water flows out of the cell. Eventually, the water loss concentrates the injected solution so that the  $\psi_s$  of the cell changes by an amount  $\Delta\psi_s = -\Delta\psi_p$ . This brings the cell back into equilibrium with the surrounding water. No further injection is required. The cell is at a permanent new  $\psi_p$ . A similar approach can be used to decrease the  $\psi_p$  except that cell solution is removed from the cell.

$$n_{sA} = \frac{-\psi_s V_A}{RT} \quad (4)$$

and the new cell volume is  $(V + V_A)$ .

### Maintaining the $\psi_p$

Increasing the  $\psi_p$  in A in Figure 1 causes  $\psi_w$  to increase. Water flows out of the cell and causes  $\psi_p$  to decrease. More cell solution is injected whenever  $\psi_p$  decreases, which maintains the  $\psi_p$  (B in Fig. 1). Each small injection adds solute, and because all the injected water is lost (volume  $V_B$ ), the cell solution becomes more concentrated. Eventually:

$$\Delta\psi_s = -\Delta\psi_p \quad (5)$$

and the cell returns to equilibrium with the external medium:

$$\psi_p + \Delta\psi_p + \psi_s + \Delta\psi_s = \psi_w = \psi_o \quad (6)$$

The volume of the cell has not changed in B and remains  $(V + V_A)$ . The amount of solute necessary to generate the  $\Delta\psi_s$  of Equation 5 is thus:

$$n_{sB} = \frac{-\Delta\psi_s(V + V_A)}{RT} \quad (7)$$

### Total Effect of Injections

From Equations 4 and 7, the total injected cell solute is  $n_{sA} + n_{sB}$  and:

$$\psi_s V_A + \Delta\psi_s(V + V_A) = \psi_s V_T \quad (8)$$

where  $V_T$  is the total volume ( $V_A + V_B$ ) of cell solution injected into the cell. Substituting into Equation 8 the  $-\Delta\psi_p$  from Equation 5 and the  $V_A$  from Equation 3, then rearranging, gives:

$$\frac{V\Delta\psi_p}{\psi_s\epsilon}(\psi_s - \Delta\psi_p - \epsilon) = V_T \quad (9)$$

This equation indicates that, for  $\epsilon$  much larger than  $\psi_s$  or  $\Delta\psi_p$ , the total injected solution is determined mostly by  $-V\Delta\psi_p/\psi_s$ .

The volume of small injections to maintain  $\psi_p$  is  $V_B = \Delta\psi_s(V + V_A)/\psi_s$  and is related to the volume  $V_A$  initially injected to change  $\psi_p$  (Eq. 3) by:

$$\frac{V_B}{V_A} = \frac{-(\epsilon + \Delta\psi_p)}{\psi_s} \quad (10)$$

Thus, for  $\epsilon$  much larger than  $\Delta\psi_p$ ,  $V_B/V_A$  is approximated by  $-\epsilon/\psi_s$ .

By this method, all the new solute remains in the cell, and only water flows out, thus making the concentration higher than before the injections. The cell returns to equilibrium with the external solution, and the  $\psi_p$  is permanently changed. To reduce  $\psi_p$ , a similar procedure is used, but solution is removed rather than injected, and water enters the cell rather than flowing out.

## MATERIALS AND METHODS

### Plant Materials

*Chara corallina* Klein ex Willd., em. R.D.W. (= *Chara australis* R. Br.) was cultivated in plastic containers (60 L) with 50 mm of soil at the bottom. The nutrient solution, changed monthly during the experiments, had a pH of 8.0 to 8.5 and was comprised of 1 mM NaCl, 0.1 mM KCl, 0.1 mM CaCl<sub>2</sub>, 0.1 mM MgCl<sub>2</sub>, and the micronutrients: 1.5 μM FeNa EDTA, 0.7 μM ZnCl<sub>2</sub>, 0.4 μM NaMoO<sub>4</sub>, 0.35 μM H<sub>3</sub>BO<sub>3</sub>, 10 nM MnCl<sub>2</sub>, 8.4 nM CoCl<sub>2</sub>, 2.3 nM CuCl<sub>2</sub>. The temperature was 22 to 24°C, and continuous fluorescent light (PAR = 15 μmol·m<sup>-2</sup>·s<sup>-1</sup>) was given at the top of the containers. The first or second internode cell from the apex of a branch of the thallus was used for determinations. The cells were 10 to 45 mm in length and 0.6 to 0.8 mm in diameter. The cells were taken from branches whose apical cells were no longer than 3 mm to ensure that the first and second internode were growing rapidly. For in situ determinations, the cells remained attached to whole plants. For single-cell determinations, the internode cells were removed by cutting on the other side of the node at each end. All measurements were conducted in the growth medium at 23°C and 15 μmol·m<sup>-2</sup>·s<sup>-1</sup> of PAR.

### In Situ Determinations

To relate the results to intact plants, elongation first was monitored in intact plants in the culture medium. Using an instrument similar to that used for soybean seedlings (31), we held the lower end of the internode rigidly with a fork made of Plexiglas and the upper end was hooked with a stainless steel wire (0.16 mm diameter) that was led to one end of an arm of a radial displacement transducer (Schaevitz, Pennsauken, NJ) situated above the culture medium. On the other end of the arm, a weight was hung from a thin plastic line that applied a force of 0.05 g to the cell. The length change of the cell was recorded by a strip chart recorder.

### Single-Cell Determinations

In most of the experiments, isolated internode cells were used. The experimental cell was excised from the plant and mounted in a horizontal Plexiglas chamber after the branches were trimmed away at each node (Fig. 2). The basal node was held in a wedge-shaped slit by an adjustable wedge plug (Fig. 2). The apical node was attached by a hook to a stainless steel wire (0.16 mm diameter) that went out of the other end of the chamber through a thin slit and connected to the arm of a horizontally arranged growth transducer (the same type as above). The chamber was covered by a piece of Plexiglas, and the interface between the chamber and the cover was sealed with petrolatum (Vaseline). The culture solution at the growth temperature flowed constantly through the chamber. The solution could be changed rapidly (3 s) by switching from one reservoir to another. The transducer was attached to a micromanipulator that does not appear in Figure 2. The system was calibrated by attaching the transducer directly to the wedge plug and varying the position of the transducer with the micromanipulator. The calibration was linear when the arm of the transducer was within ±7.5° of the central position for the growth transducer.

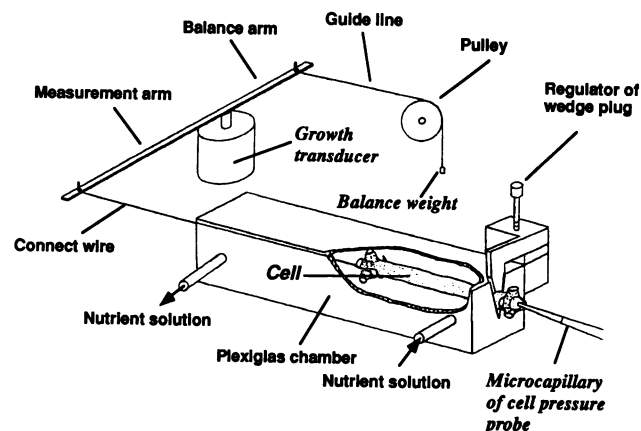


**Figure 2.** Apparatus for simultaneously determining elongation and  $\psi_p$  in a single internode cell of *C. corallina*. Elongation is detected with the growth transducer, and  $\psi_p$  is detected with the cell pressure probe. The  $\psi_p$  can be permanently changed (clamped) with the pressure probe, as described for Figure 1. For details, see "Theory" and "Materials and Methods."

The tip of the microcapillary of the cell pressure probe (39) was inserted into the cell at the stationary node by using a micromanipulator. The orifice of the tip of the microcapillary was opened and sharpened with a grinder (Narashige, Optical Apparatus, Ardmore, PA) to give a short, sharp tip with a diameter of 30 to 50 μm. The large tip prevented plugging and caused little wounding. During grinding, the microcapillary was held by a micromanipulator and kept at an angle that made a sharpened face at about 45° to the long axis. The sharpened microcapillary was dipped in silicone oil and exposed to hot air from a hair dryer to make a dry but hydrophobic outer surface. The shape and hydrophobic treatment reduced leakage when the tip was inserted into a cell (leakage detected by a decrease in the  $\psi_p$ ).

A large cell pressure probe was used for the turgor clamp. We used 3.5 mm<sup>3</sup> of the inner regulatable reservoir for cell solution. The remaining internal volume was occupied by silicone oil. For measurements involving increased  $\psi_p$ , cell solution was first obtained from another similar cell. The tip was inserted in the test cell, and the  $\psi_p$  was measured by returning the oil/solution boundary to the position before insertion. The  $\psi_p$  was then raised as described before (see "Theory" and Fig. 1). For measurements involving decreased  $\psi_p$ , the  $\psi_p$  was measured and the tip was withdrawn slightly from the cell to allow a leak. It was resealed into the cell when the  $\psi_p$  decreased to the desired level. The  $\psi_p$  was kept at this level by removing small quantities of cell solution until there was no further change (see "Theory" and Fig. 1).

The inner diameter of the microcapillary was 0.56 mm, and the position of the meniscus could be observed to at least 0.1 mm at ×50 magnification with the stereomicroscope. This allowed a volume to be detected of less than ×0.0003 to ×0.001 of cell volume. Both the elongation and the  $\psi_p$  were continuously recorded with a two-pen chart recorder.

### $\epsilon$ , $L_p$ , and $\psi_s$

The  $\epsilon$  and  $L_p$  of growing and mature internode cells were measured by the methods of Zimmermann and Steudle (43).

The cell volume and surface area were determined from the lengths and widths of the cells determined microscopically. After determining these parameters, we cut off one end of the cell, a drop of cell solution was quickly collected, and  $\psi_s$  was measured using a microliter isopiestic psychrometer (3). The osmotic potential of the culture medium also was measured with the same psychrometer.

## RESULTS

### Growth-Induced Water Potential, $\epsilon$ , and $L_p$

Table I shows that the  $\psi_p$  essentially equalled  $-\psi_s$  in growing internode cells of *Chara*. Also, the  $\psi_w$  of the cells was almost the same as the  $\psi_o$  of the culture medium. This indicates that the growth-induced water potential ( $\psi_o - \psi_w$ ) was negligible (2), the cells were in near-equilibrium with  $\psi_o$ , and the conditions of Equation 2 were satisfied. The growth-induced water potential was small because the  $L_p$  of the cells was large,  $0.87$  to  $1.4 \times 10^{-6} \text{ m} \cdot \text{s}^{-1} \cdot \text{MPa}^{-1}$ , and the rate of water influx for growth was slow (about  $10^{-10} \text{ m} \cdot \text{s}^{-1}$ ), which gives a calculated ( $\psi_o - \psi_w$ ) on the order of only  $0.0001 \text{ MPa}$ . The  $\epsilon$  was large and ranged between  $21$  and  $83 \text{ MPa}$  whether or not the cells were growing. The  $\psi_s$  was  $-0.60$  to  $-0.62 \text{ MPa}$ , the cell volume was  $6$  to  $18 \times 10^{-9} \text{ m}^3$ , and the surface area was  $3$  to  $12 \times 10^{-5} \text{ m}^2$ .

### Excision Effects

Before excision, growth rates in the intact plants were measured in the culture medium and were steady for  $20 \text{ h}$  (Fig. 3A). Excising, transporting, and puncturing the internodes with the pressure probe shown in Figure 2 had little effect on their growth rate. Growth ordinarily was slightly faster for about  $20 \text{ min}$  and then recovered to a rate similar to that before excision (Fig. 3, B and C). Growth remained constant for at least  $8$  to  $10 \text{ h}$  (Fig. 3, B–D). The rate varied widely from  $30$  to about  $200 \mu\text{m/h}$ , depending on the cell, but was not related to cell length. Puncturing the cell with the pressure probe sometimes reduced the growth rate (Fig. 3C) and sometimes did not (Fig. 3D), but the rate was always stable afterward. Because growth was similar to that of the intact plant and remained stable for a long time in the single-cell apparatus, all the following experiments were conducted in the single-cell apparatus (Fig. 2).

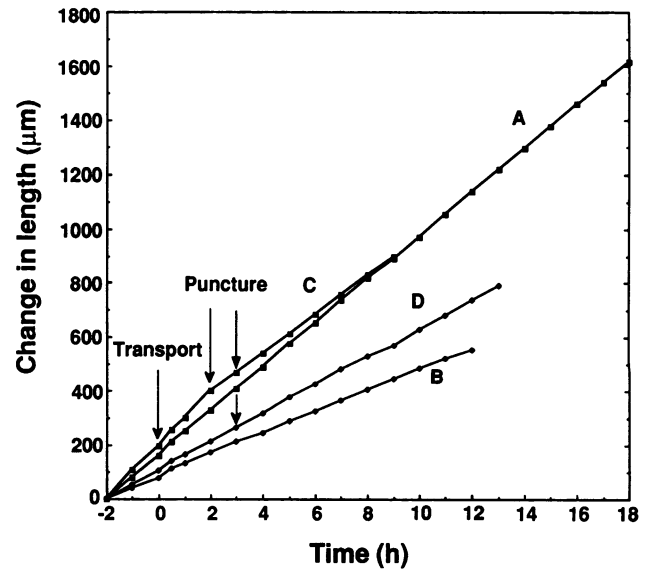


**Figure 3.** Growth of *Chara* internode cells in situ (A), after excision and transport to the single-cell apparatus described in Figure 2 (B–D), and after puncturing with the microcapillary of the pressure probe in the single-cell apparatus (C and D). The transport of the cells from in situ to the apparatus took  $20$  to  $30 \text{ s}$ . The original cell lengths were  $32$ ,  $40$ ,  $28$ , and  $21 \text{ mm}$ , respectively, for cells A, B, C, and D. Transport and puncture took place at the arrows.

### Turgor Clamp and Elongation

A stable  $\psi_p$  of  $0.5$  to  $0.7 \text{ MPa}$  was obtained when the tip of the microcapillary was inserted into an internodal cell. If cell solution was injected or removed, the  $\psi_p$  quickly returned to near its original level (half-time of  $3$ – $6 \text{ s}$ , Table I, and Fig. 4, right). If the injection was followed with many small injections,  $\psi_p$  was maintained at the new level, and no further injections were required after about  $20 \text{ min}$  (Fig. 4, left) as predicted from "Theory." During the injections,  $\psi_p$  initially varied around the mean by  $\pm 0.005 \text{ MPa}$  but varied less as injections proceeded.

After a  $\psi_p$  change, growth and the new  $\psi_p$  remained stable for hours. Following a  $\psi_p$  step up, there was an immediate increase in length followed by a steady elongation monitored for almost  $5 \text{ h}$  in the experiment of Figure 5. The rate of

**Table I.** Potentials, Hydraulic Parameters, and Dimensions of Growing and Mature Internode Cells of *Chara* Typical of Those Used in the Experiments

The  $\psi_o - (\psi_p + \psi_s) = (\psi_o - \psi_w)$  = water potential difference across cell membranes that in growing cells is induced by growth, and  $n$  = number of cells. Growth was  $35$  to  $180 \mu\text{m/h}$  in growing cells and  $0 \mu\text{m/h}$  in mature cells. The  $\psi_p$  and  $t_{1/2}$  were determined with the cell pressure probe. The  $\psi_s$  and  $\psi_o$  were measured with a microliter isopiestic psychrometer. Data for potentials are means  $\pm 1 \text{ SD}$ . Data for hydraulic parameters and dimensions are ranges.

	$\psi_o$	$\psi_s$	$\psi_o - (\psi_p + \psi_s)$	$\epsilon$	$L_p$	$t_{1/2}$	$V$	$A$	$n$	
	MPa	MPa	MPa	MPa	$\text{m} \cdot \text{s}^{-1} \cdot \text{MPa}^{-1}$	s	$\text{m}^3$	$\text{m}^2$		
Growing	$0.58$ $\pm 0.06$	$-0.60$ $\pm 0.05$	$-0.01$ $\pm 0.00$	$0.01$ $\pm 0.01$	$21$ to $80$	$0.87$ – $1.4 \times 10^{-6}$	$3.5$ – $6.0$	$5.7$ – $17.3 \times 10^{-9}$	$2.8$ – $11.3 \times 10^{-5}$	$5$
Mature	$0.61$ $\pm 0.05$	$-0.62$ $\pm 0.05$	$-0.01$ $\pm 0.00$	$0.00$ $\pm 0.00$	$33$ to $83$	$0.90$ – $1.2 \times 10^{-6}$	$3.0$ – $6.0$	$14.3$ – $17.6 \times 10^{-9}$	$7.6$ – $11.7 \times 10^{-5}$	$4$

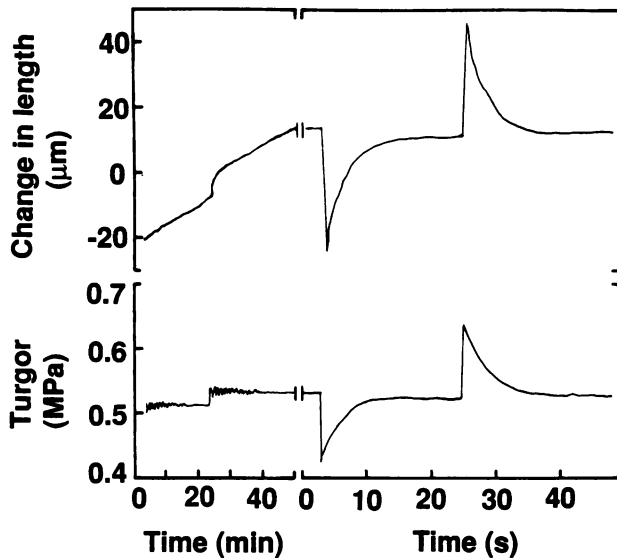


**Figure 4.** Turgor clamp and elongation (left) and  $\psi_p$  and length relaxation after single injection/uptake (right) in the same *Chara* internode cell in the apparatus in Figure 2. No turgor clamp was used in the experiment on the right. Note the change in the x axis at 50 min. Initially, cell length was 25 mm, growth rate was 35  $\mu\text{m}/\text{h}$ , and  $\psi_p$  was 0.62 MPa.

elongation after the step up was the same as before the step up. After about 20 min of injections, the  $\psi_p$  continued at the new level without the necessity for further injections and thus had been “permanently” changed.

Because of the limited capacity of the pressure probe, the turgor clamp was operated in two  $\psi_p$  ranges: 0.2 to 0.5 and 0.4 to 0.8 MPa. In the lower range, there was a switch-like threshold  $\psi_p$  for growth, normally approximately 0.3 to 0.4 MPa (Fig. 6). Below this threshold, no growth was observed (Fig. 6, steps 2–4).  $\psi_p$  downshifts caused an initial elastic shrinkage, and equivalent upshifts caused an equivalent elastic stretching (Fig. 6, steps 2–4). Above the threshold, the same elastic behavior was observed, but it was combined with a steady elongation observable after 5 to 25 min (Fig. 6, steps 0, 1, 5–8). The elongation resumed at the same rate after the initial extension/shrinkage regardless of the  $\psi_p$  as long as  $\psi_p$  was above the threshold (Fig. 6, steps 0, 1, 5–8). Less time was required between the initial elastic response and the final growth response when  $\psi_p$  was slightly above the threshold than when it was far above. We were unable to detect any evidence of plastic deformation in this  $\psi_p$  range.

In the higher  $\psi_p$  range, growth also was unaltered by variations in  $\psi_p$  up to those slightly above the maximum obtainable by the cell (slightly above 0.56 MPa, Fig. 7, curve A, steps 1 and 3). The cells elongated rapidly when  $\psi_p$  was at its original level (Fig. 7, step 0) and resumed at the same rate following the elastic response to  $\psi_p$  steps up or down (Fig. 7, steps 0–2). When the  $\psi_p$  was stepped up to a level substantially higher than the maximum attainable by the cell (Fig. 7, step 4), the growth increased above the original rate as though plastic deformation was beginning. However, the growth often was not steady (data not shown), and growth

did not occur when the  $\psi_p$  was returned to the prior level (Fig. 7, step 5, observed for 6 h). Despite repeated attempts, we never observed a growth recovery after exposure to  $\psi_p$  high enough to cause plastic deformation.

The duration of the initial extension/shrinkage could be determined by subtracting the steady growth rate (Fig. 7B, steps 0–3) from the observed changes in length (Fig. 7A). This subtraction indicates that the extension/shrinkage was complete in about 25 min at high  $\psi_p$  (Fig. 7C).

Figure 8A shows the relationship between growth and  $\psi_p$  in a single cell in which the entire range of  $\psi_p$  was possible to obtain because of an unusually small difference between the original and threshold turgors (0.11 MPa). Cell growth remained independent of  $\psi_p$  over the entire range. Figure 8B shows similar behavior in four different cells, one of which covered almost the whole  $\psi_p$  range. In every case, growth began abruptly at the  $\psi_p$  threshold but was unaffected over the range of  $\psi_p$  encountered by the cells. When  $\psi_p$  was substantially (0.08 MPa) above the original, however, a  $\psi_p$  dependency appeared (Fig. 8B), but growth was often transitory and did not resume when  $\psi_p$  was lowered (as in Fig. 7, steps 4 and 5).

We explored more fully the significance of the transition between the initial elastic stretching and the subsequent steady growth by investigating nongrowing cells. Nongrowing cells were obtained by exposing growing cells to various inhibitors. Figure 9 shows that inhibitors of photosynthesis (DCMU) and energy-dependent phosphorylation (FCCP), when added together (5  $\mu\text{M}$  + 5  $\mu\text{M}$ ) in the light, inhibited growth immediately. After 20 min, growth became zero.  $\psi_p$  was not altered for about 2 h. After 2 h,  $\psi_p$  decreased, and the cells shrank presumably because of losses in membrane selectivity.

When growth was inhibited but the membrane had not yet lost selectivity,  $\psi_p$  jumps resulted in an initial rapid deformation followed by a slow approach to a stable length

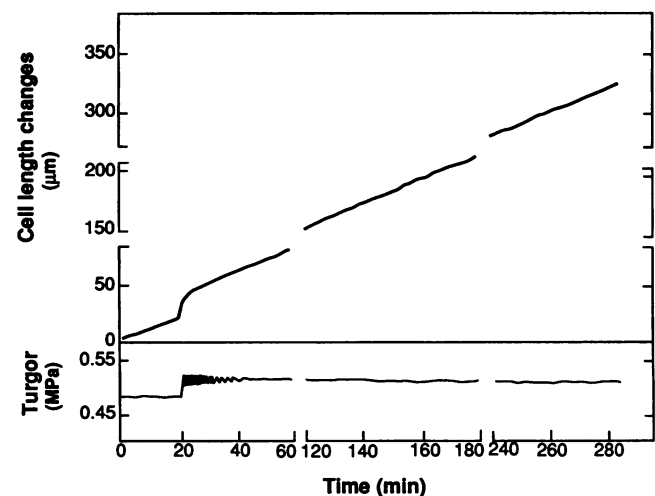


**Figure 5.** Elongation of *Chara* internode cells at various times after a step up in  $\psi_p$  with the turgor clamp in the apparatus shown in Figure 2. Note breaks in x and y axes. The cell initially was 34 mm long.

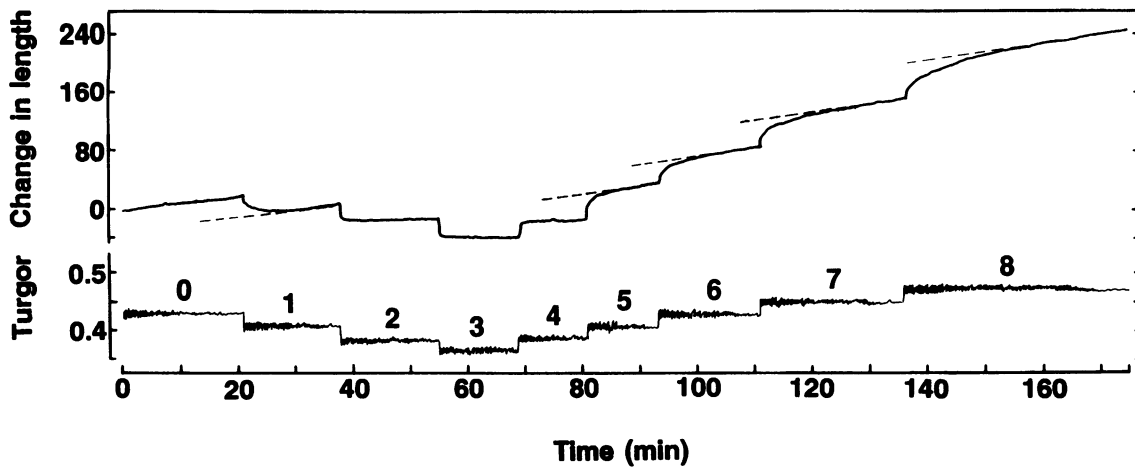


**Figure 6.** Elongation of *Chara* internode cells in response to various  $\psi_p$  step changes with the turgor clamp in the low  $\psi_p$  range. Before time zero, several steps down were used to decrease the  $\psi_p$  to about 0.43 MPa with the turgor clamp. Dashed lines show the resumption of steady growth after each subsequent  $\psi_p$  step. Initially, the cell length was 42 mm, growth rate was 64  $\mu\text{m}/\text{h}$ , and  $\psi_p$  was 0.5 MPa.

resembling the kinetics seen in growing cells below the  $\psi_p$  threshold (Fig. 10A). Similar responses were seen in mature cells (Fig. 10B) and in growth-inhibited cells whose  $\psi_p$  was varied with an osmoticum (Fig. 10C).

The respiratory inhibitor dinitrophenol (5–10  $\mu\text{M}$ ) in the dark generally caused effects similar to DCMU and FCCP in the light. Other inhibitors such as monensin (5–10  $\mu\text{M}$ ) caused immediate irreversible  $\psi_p$  loss and were not used further.

**$\psi_p$  Changes Induced by Osmotica and Turgor Clamp**

Because previous investigators often used osmotica to vary the  $\psi_p$  in growing cells (18), we compared the effects of

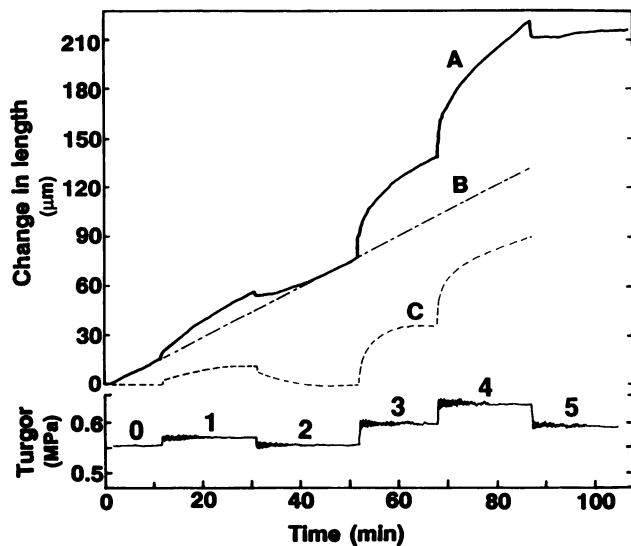


**Figure 7.** Elongation of *Chara* internode cells in response to  $\psi_p$  step changes with the turgor clamp in the high  $\psi_p$  range. Measurements were made around and above the normal  $\psi_p$  of the cell. A shows changes in cell length, B shows the slope of the length change in A (from  $\psi_p$  steps 0–3), and C is A – B. Initially, the cell length was 29 mm, growth was 92  $\mu\text{m}/\text{h}$ , and  $\psi_p$  was 0.56 MPa.

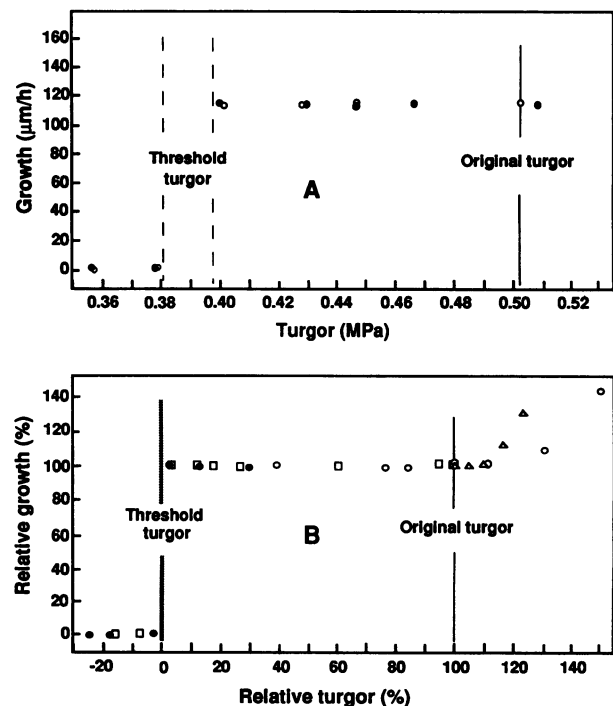


**Figure 8.** Growth at various  $\psi_p$  in internode cells of *Chara*. A, Data from a single cell, in which  $\circ$  was measured during  $\psi_p$  steps down and  $\bullet$  was measured during  $\psi_p$  steps up in the same cell. The x axis shows the actual  $\psi_p$ , and the y axis shows the absolute growth rate. B, Data from four different cells ( $\circ$ ,  $\square$ ,  $\bullet$ ,  $\Delta$ ). The x axis shows the relative  $\psi_p$  with the threshold as 0% and the original  $\psi_p$  (before turgor clamping) as 100% for each cell. The y axis is the relative growth rate (as percentage of the initial elongation before the turgor clamp was used).

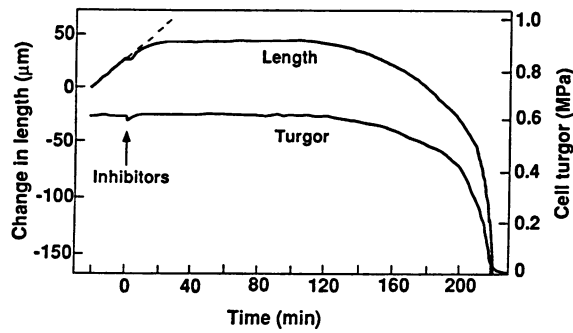


**Figure 9.**  $\psi_p$  and elongation in *Chara* internode cell at various times after inhibitors DCMU and FCCP ( $5 \mu\text{M} + 5 \mu\text{M}$ ) were added to the external medium in the light. Dashed line shows elongation expected if inhibitors had no effect on rate.

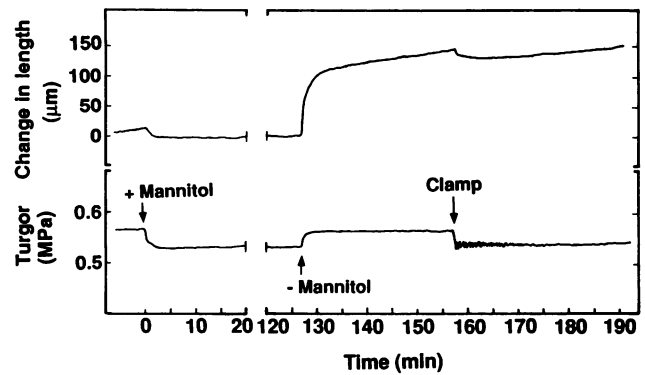


**Figure 11.** Comparison of turgor clamp and osmoticum (mannitol) with the same *Chara* internode cell. Cell was first exposed to  $-0.05$  MPa mannitol for about 2 h (note break in x axis) and then returned to original culture medium after which the  $\psi_p$  was decreased 0.05 MPa with the turgor clamp (cell length was 44 mm).

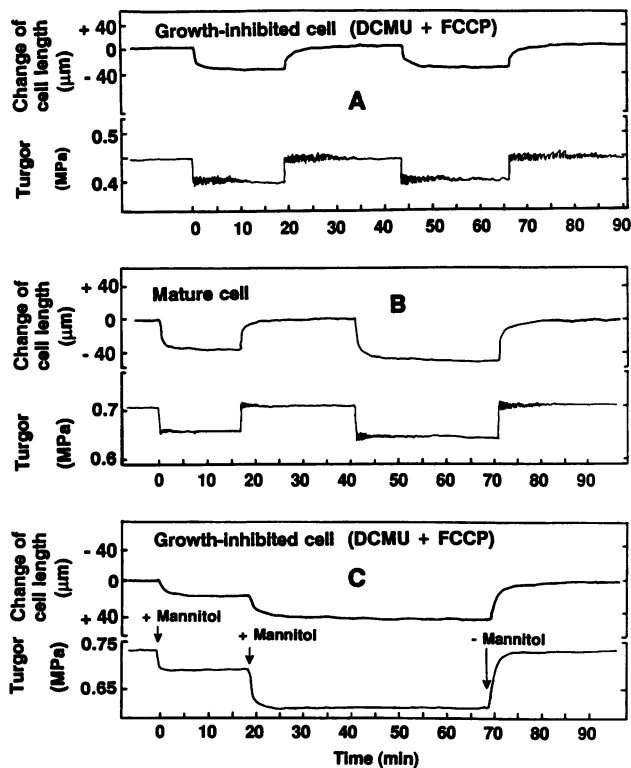


**Figure 10.** Length and  $\psi_p$  in nongrowing internode cells of *Chara*. A, Growing cell after inhibiting growth with  $5 \mu\text{M}$  DCMU +  $5 \mu\text{M}$  FCCP in the light and changing  $\psi_p$  0.05 MPa with the turgor clamp (growth before inhibition was  $92 \mu\text{m}/\text{h}$ , length was 28 mm). B, Mature cell having  $\psi_p$  changed 0.05 MPa with the turgor clamp (growth before clamping was  $0 \mu\text{m}/\text{h}$ , length was 45 mm). C, Growing cell after inhibiting growth with  $5 \mu\text{M}$  DCMU +  $5 \mu\text{M}$  FCCP in the light and changing  $\psi_p$  with mannitol (growth before inhibition was  $68 \mu\text{m}/\text{h}$ , length was 41 mm). This cell was first exposed to  $-0.03$  MPa mannitol (+mannitol), then to  $-0.06$  MPa mannitol (-mannitol), and finally was returned to the original medium (-mannitol).

osmotica and turgor clamping. Figure 11 shows that the methods gave different results. Growth resumed partially or not at all when  $\psi_p$  was stepped down in a growing cell with mannitol (Fig. 11, note break in x axis). On the other hand, the same  $\psi_p$  step down with the turgor clamp in the same cell was not inhibitory, and growth resumed at a rate similar to that before clamping (Fig. 11). Sucrose showed comparable effects (data not shown). With KCl, the result was intermediate between mannitol and the turgor clamp. Growth was inhibited but eventually resumed after longer times than with the turgor clamp (Fig. 12). With both mannitol and KCl, removal of the osmoticum caused a large burst in enlargement not seen with the turgor clamp (Figs. 11 and 12, see also Figs. 6 and 7). Green et al. (18) reported the same kind of inhibition with exposure to osmoticum and a similar burst of elongation with removal of osmoticum.

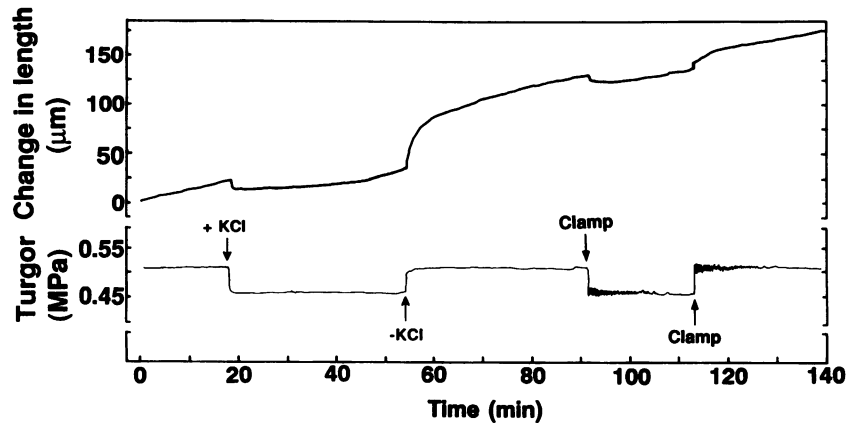
## DISCUSSION

The turgor clamp showed that small  $\psi_p$  changes could start or stop growth with almost a switch-like action. The start/stop signal could operate repeatedly. The  $\psi_p$  range for the signal was narrow, about 0.01 MPa, and invariant. Thus,  $\psi_p$  needed to be above a threshold that was essential for the growth process. We will call this  $\psi_p$ , the turgor threshold for growth.

In mature cells, this response was absent. There was only an initial immediate deformation (elastic) followed by a gradual deformation that required 5 to 25 min for completion (viscoelastic). When the  $\psi_p$  was returned to the previous level, the cell dimensions returned to their previous level. A similar response was observed if growing cells were exposed to inhibitors that prevented growth or if growing cells were subjected to  $\psi_p$  below the threshold. The elastic effects were in every way like those of the mature cells. Thus, regardless of whether or not the cells could grow, their walls exhibited reversible elastic behavior typical of many solid materials (12).

Elastic/viscoelastic behavior is generally attributable to a reversible straightening of individual polymer molecules un-

**Figure 12.** Comparison of turgor clamp and osmoticum (KCl) with the same *Chara* internode cell. Cell was first exposed to  $-0.05$  MPa KCl and then returned to original culture medium after which the  $\psi_p$  was decreased  $0.05$  MPa with the turgor clamp (cell length was  $23$  mm).



der tension that is instantaneous in an ideal polymer but may require time in a polymer having complex coiling or intermolecular bonding. The longer times to complete the effects at high  $\psi_p$  than at low  $\psi_p$  is consistent with the straightening of more complex coiling as the tension increases. The reversibility of the effects is diagnostic for elastic/viscoelastic phenomena and was clearly evident here.

Above the threshold, elasticity was apparent, but a steady growth was superimposed on it and could be observed after the elastic responses were completed. Regardless of the direction of the  $\psi_p$  change, steady growth resumed at the rate before the pressure jump. Because the elastic/viscoelastic changes were rapidly reversible but growth was not, growth could be clearly distinguished from elastic behavior.

With osmotica, the two effects were more difficult to separate. Osmotica caused an elastic shrinkage followed by a large spurt in cell length when the solutes were removed. Previous workers also observed this effect (33), and some considered it to be caused in part by growth occurring but unexpressed when solute was present (33). On the other hand, Green et al. (18) and Ortega et al. (32) suggested that there was an immediate yield point just below the  $\psi_p$  of the cell (about  $0.03$  MPa) that changed in a way that could compensate for some of the  $\psi_p$  changes and in this way cause a growth spurt when the solutes were removed. They observed no elastic shrinkage when  $\psi_p$  decreased (18). Because the elastic and viscoelastic properties of cell walls are well known (6, 11, 23, 33, 41) and were confirmed by the turgor clamp, it seems impossible that there is no shrinking when a cell experiences a  $\psi_p$  step down unless growth occurs at the same time and cancels the shrinkage. The net effect would be a temporary apparent cessation of growth similar to that suggested by Cleland (11), but, because growth would be occurring but unseen, the cells would not be at an immediate yield point. The hidden growth would be apparent when  $\psi_p$  recovered, as we observed with the turgor clamp. Therefore, the early cessation of growth after a  $\psi_p$  step down was not consistent with a changing yield threshold. In addition, no growth burst was observed with the turgor clamp after a  $\psi_p$  step up. Therefore, the subsequent resumption of growth also was not consistent with a changing yield threshold. These results make it unlikely that the yield threshold varied.

Osmotica inhibited growth, which was unmistakable when

close comparisons were made in the same cell with the same  $\psi_p$  change caused either by osmoticum or the turgor clamp. The only differences between the two experiments were the presence or absence of external solute and the direction of change in the internal osmotic potential. As  $\psi_p$  decreased with exposure to an osmoticum, the cell contents became more concentrated. As  $\psi_p$  decreased with the turgor clamp, the cell contents became more dilute. Because the  $\psi_p$  was identical in the two cases, the only possible effect of these changes was on metabolism. However, the turgor clamp gave the same growth rates during  $\psi_p$  steps down (dilution) and steps up (concentration), which indicates that any metabolic effects were too small to affect the measurements. Thus, external osmotica appeared to cause direct interactions with the wall or plasmalemma that were absent when  $\psi_p$  was changed with the turgor clamp. This concept is strengthened by the solute-specific nature of the inhibition. Sucrose and mannitol were more inhibitory than KCl. Sugars and their analogs can change wall properties and inhibit wall enzymes (22, 29). These possible side effects indicate that external osmotica should be avoided when studying  $\psi_p$  effects on cell growth.

Since the model of  $\psi_p$ -driven growth was set up by Lockhart (27, 28), it has been thought that the growth of plant cells is mainly a plastic or viscoplastic deformation of walls caused by  $\psi_p$ . It is well known for polymers that plastic effects require time and are irreversible, often exhibiting a rapid phase followed by a slow steady "creep" or viscoplastic phase. Finally, strain hardening occurs that decreases creep.

Viscoplastic behavior is thought to result from a sliding of polymers past each other so that an overall lengthening of the material occurs. Because of the sliding, release of the external force does not reverse the lengthening. This nonreversibility can be diagnostic for plastic effects in a nonliving system. The rapid phase is probably caused by sliding of weak bonds and the creep phase by stronger bonds. Strain hardening indicates that slide-prone bonds have been exhausted.

There are two consequences of this mechanism. First, the rate of deformation must change as the  $\psi_p$  changes. Thus, it is noteworthy that growth did not change between the  $\psi_p$  threshold and the maximum  $\psi_p$  attainable at the  $\psi_s$ . Second, in the absence of metabolism, steady plastic deformation



(creep) should continue for a time but should eventually decrease as the polymer undergoes strain hardening. However, we were unable to detect unaltered growth rates when metabolism was inhibited. The immediate decrease in growth despite a constant  $\psi_p$  indicates that growth was more closely determined by energy metabolism than by detectable effects of creep. It follows that between the  $\psi_p$  threshold and the maximum cell  $\psi_p$ , plastic deformation played little if any role in growth.

Others also observed growth responses that are consistent with this conclusion. Shackel et al. (37) reported that leaves grew at a constant rate under environmental conditions that caused  $\psi_p$  to change in the epidermal cells. Green et al. (18) noted a considerable  $\psi_p$  range over which growth occurred at a constant rate. In both studies  $\psi_p$  was measured directly and thus especially compelling measurements were provided, although the osmotica used in one of them (18) may have caused side effects.

The constancy of growth at variable  $\psi_p$  and the dependence on metabolism imply that there could be a metabolically controlled differential sliding of wall microfibrils that only occurred under tension and required metabolism. There is evidence that wall enzymes are involved in growth (16, 17, 21, 24, 29). These activities probably create a demand for metabolic energy to supply new wall materials (polysaccharides and proteins) and also for the assembly of the materials into walls (4, 5, 7, 11, 14, 15, 24, 33, 36, 40). This energy could be essential for the metabolic reactions actually causing growth (17, 19, 34).

It is interesting that, when  $\psi_p$  was forced above the maximum attainable by the cell, there was an increase in elongation rate with increased  $\psi_p$  that resembled the behavior of a polymer undergoing plastic deformation. A similar response was noted by Ortega et al. (32). Thus, it was possible to observe wall behavior that conformed to the concept of  $\psi_p$ -driven plastic elongation with the turgor clamp. This gives confidence that we would have detected it if it had been present at the lower  $\psi_p$  in the normal range. Its absence except at abnormally high  $\psi_p$  indicates that experiments involving deformation of nonliving tissue (9, 10, 25, 42) or isolated cell walls (19, 35) may need to be reinterpreted because the observed plastic behavior may have been outside the possible  $\psi_p$  range for the cells. This suggests that experiments with one-dimensional force applied to  $\psi_p$ -containing cells and tissues (13, 31) also may display plastic behavior because they apply forces above the normal cell  $\psi_p$ .

At these abnormally high turgors, the plastic deformation inhibited growth after the initial deformation. This suggests that there could have been damage to a structural feature necessary for growth. Exceeding the normal stretch of cells may damage the fine structure of the membrane and/or microtubules likely to be involved in the biosynthesis of the walls (26). This wound effect did not disturb the  $\psi_p$  and thus was not a simple loss of membrane selectivity.

With the turgor clamp, we were able to explore the entire range of turgors from those too low to support growth to those so high that wounding occurred. There was some disturbance of growth when the cells were excised, transported, and punctured, but recovery was rapid, and growth resumed at rates similar to those of intact cells for long times

(as long as 25 h). A similar response was observed in another laboratory (32). The possibility that the probe directly altered the metabolic activity of the cell seems remote in view of this growth response, but changing the  $\psi_p$  could have caused metabolic effects that would normally take place.

*C. corallina* was an ideal species for this work because it shows no activity for  $\psi_p$  regulation, and osmoregulation is slow (1). The turgor clamp permanently changed the  $\psi_p$  of the cells, which remained stable for many hours after injections ceased. A stable  $\psi_p$  was not achievable with only one injection and normally required several hundred repeated but diminishing injections to bring the  $\psi_s$  into balance with the new  $\psi_p$  (see "Theory"). Assuming the cells had a  $\Psi_s$  of  $-0.6$  MPa and  $\epsilon$  of 50 MPa (Table I), increasing the  $\psi_p$  by 0.1 MPa required the injection of a cell solution having a volume 0.2% of the cell volume (Eq. 3), which is negligibly small. To maintain the new  $\psi_p$ , an additional cell solution having a volume of 16.7% of cell volume needed to be injected (Eq. 10). Water moved out of the cell during these maintenance injections, but thereafter, no further water movement was caused by the turgor clamp, and the cell returned to its usual equilibrium state. In this equilibrium state with the external medium, a concentration difference remained between the cell solution in the probe and in the clamped cell, but no effects on cell behavior were detected. The injections served to indicate that the pressure probe was in hydraulic contact with the cell interior, and indeed, a stable pressure not requiring injections indicated that the microcapillary tip was blocked. This problem plagued the efforts of Ortega et al. (32) but was avoided by using a large orifice tip in the present work.

A central question concerning cell enlargement has been the role of water uptake,  $\psi_p$ , and metabolism. In higher plants, the hydraulic conductance of the path for water movement is complex and requires a significant water potential difference between the water in the xylem and the enlarging cells to supply water to the cells (2, 30, 31). In *Chara*, the water supply was not a limiting factor for the internodal cells, which were surrounded directly by the water source. The hydraulic conductivity of the cells was so high that water potential differences were negligible.  $\psi_p$ , although necessary for growth, did not drive it according to the rules of physical deformation. The role of  $\psi_p$  was restricted to placing the wall under a strain large enough to allow growth to occur, but the rate appeared to be controlled by factors other than  $\psi_p$ . The present results suggest that wall metabolism may supply these factors and, in the absence of a significant frictional resistance to water movement, may be the major determinant of the rate of growth.

#### NOTE ADDED IN PROOF

During a recent visit to our laboratory, Professor Mary A. Bisson observed protoplasmic streaming in *Chara corallina* internodes before, during, and after inserting the microcapillary. She also found that streaming continued during pressure steps with the turgor clamp. These observations further indicate that the manipulations with the turgor clamp caused minimal wounding.

## ACKNOWLEDGMENTS

We thank Dr. Roger Spanswick at Cornell University for kindly supplying the initial culture of *Chara* and Dr. Hiroshi Nonami for subculturing the plants.

## LITERATURE CITED

1. **Bisson MA, Bartholomew D** (1984) Osmoregulation or turgor regulation in *Chara*? *Plant Physiol* **74**: 252–255
2. **Boyer JS** (1985) Water transport. *Annu Rev Plant Physiol* **36**: 473–516
3. **Boyer JS, Knipling EB** (1965) Isopiestic technique for measuring leaf water potentials with a thermocouple psychrometer. *Proc Natl Acad Sci USA* **54**: 1044–1051
4. **Brummell DA, Hall JL** (1983) Regulation of cell wall synthesis by auxin and fusicoccin in different tissues of Pea stem segments. *Physiol Plant* **59**: 627–634
5. **Brummell DA, Hall JL** (1985) The role of cell wall synthesis in sustained auxin-induced growth. *Physiol Plant* **63**: 406–412
6. **Burström HG, Uhrström I, Wurscher R** (1967) Growth, turgor, water potential, and Young's modulus in pea internodes. *Physiol Plant* **20**: 213–231
7. **Carpita NC** (1984) Cell wall development in maize. *Plant Physiol* **76**: 205–212
8. **Cleland RE** (1959) Effect of osmotic concentration on auxin-action and on irreversible and reversible expansion of the *Avena* coleoptile. *Physiol Plant* **12**: 809–825
9. **Cleland RE** (1967) A dual role of turgor pressure in auxin-induced cell elongation in *Avena* coleoptile. *Planta* **77**: 182–191
10. **Cleland RE** (1967) Extensibility of isolated cell walls: measurement and changes during cell elongation. *Planta* **74**: 197–209
11. **Cleland RE** (1971) Cell wall extension. *Annu Rev Plant Physiol* **22**: 197–222
12. **Courtney TH** (1990) *Mechanical Behavior of Materials*. McGraw-Hill Publishing Co, New York
13. **Cramer GR, Bowman DC** (1992) Kinetics of maize leaf elongation. I. Increased yield threshold limits short-term, steady-state elongation rates after exposure to salinity. *J Exp Bot* **43**: 857–864
14. **Fry SC** (1986) Cross-linking of matrix polymers in the growing cell walls of angiosperms. *Annu Rev Plant Physiol* **37**: 165–186
15. **Fry SC** (1988) *The Growing Plant Cell Wall: Chemical and Metabolic Analysis*. Longman Scientific and Technical, John Wiley & Sons, New York
16. **Fry SC** (1989) The structure and functions of xyloglucan. *J Exp Bot* **40**: 1–11
17. **Fry SC** (1989) Cellulases, hemicelluloses and auxin-stimulated growth: a possible relationship. *Physiol Plant* **75**: 532–536
18. **Green PB, Erickson RO, Buggy J** (1971) Metabolic and physical control of cell elongation rate. In vivo studies in *Nitella*. *Plant Physiol* **47**: 423–430
19. **Haughton PM, Sellen DB** (1969) Dynamic mechanical properties of the cell wall of some green algae. *J Exp Bot* **20**: 516–535
20. **Haughton PM, Sellen DB, Preston RD** (1968) Dynamic mechanical properties of the cell wall of *Nitella opaca*. *J Exp Bot* **19**: 1–12
21. **Hoson T, Nevins DJ** (1989)  $\beta$ -D-Glucan antibodies inhibit auxin-induced cell elongation and changes in the cell wall of *Zea* coleoptile segments. *Plant Physiol* **90**: 1353–1358
22. **Hughes R, Street HE** (1974) Galactose as an inhibitor of the expansion of root cells. *Ann Bot* **38**: 555–564
23. **Kamiya N, Tazawa M, Takata T** (1963) The relation of turgor pressure to cell volume in *Nitella* with special reference to mechanical properties of the cell wall. *Protoplasma* **57**: 501–521
24. **Keegstra K, Talmadge KW, Bauer WD, Albersheim P** (1973) The structure of plant cell walls. III. A model of the walls of suspension-cultured sycamore cells based on the interconnections of the macromolecular components. *Plant Physiol* **51**: 188–196
25. **Kutschera U, Schopfer P** (1986) *In-vivo* measurement of cell-wall extensibility in maize coleoptiles: effects of auxin and abscisic acid. *Planta* **169**: 437–442
26. **Lloyd CW** (1984) Toward a dynamic helical model for the influence of microtubules on wall patterns in plants. *Int Rev Cytol* **86**: 1–51
27. **Lockhart JA** (1965) An analysis of irreversible plant cell elongation. *J Theor Biol* **8**: 264–275
28. **Lockhart JA** (1965) Cell extension. In J Bonner, JE Varner, eds, *Plant Biochemistry*, Academic Press, New York, pp 826–849
29. **Nagahashi G, Tu SI, Fleet G, Namgoong SN** (1990) Inhibition of cell wall-associated enzymes in vitro and in vivo with sugar analogs. *Plant Physiol* **92**: 413–418
30. **Nonami H, Boyer JS** (1990) Primary events regulating stem growth at low water potentials. *Plant Physiol* **93**: 1601–1609
31. **Nonami H, Boyer JS** (1990) Wall extensibility and cell hydraulic conductivity decrease in enlarging stem tissues at low water potentials. *Plant Physiol* **93**: 1610–1619
32. **Ortega JKE, Zehr EG, Keanini RG** (1989) In vivo creep and stress relaxation experiments to determine the wall extensibility and yield threshold for the sporangiophores of *Phycomyces*. *Biophys J* **56**: 465–475
33. **Preston RD** (1974) *The Physical Biology of Plant Cell Walls*. Chapman and Hall, London, UK
34. **Preston RD** (1979) Polysaccharide conformation and cell wall function. *Annu Rev Plant Physiol* **30**: 55–78
35. **Probine MC, Preston RD** (1962) Cell growth and the structure and mechanical properties of the wall in internodal cells of *Nitella opaca*. II. Mechanical properties of the walls. *J Exp Bot* **13**: 111–127
36. **Ray PM** (1967) Autoradiographic study of cell wall deposition in growing plant cells. *J Cell Biol* **35**: 659–674
37. **Shackel KA, Matthews MA, Morrison JC** (1987) Dynamic relation between expansion and cellular turgor in growing grape (*Vitis vinifera* L.) leaves. *Plant Physiol* **84**: 1166–1171
38. **Steudle E** (1989) Water flow in plants and its coupling to other processes: an overview. *Methods Enzymol* **174**: 183–225
39. **Steudle E, Zimmermann U** (1974) Determination of the hydraulic conductivity and of reflection coefficients in *Nitella flexilis* by means of direct cell-turgor pressure measurements. *Biochim Biophys Acta* **332**: 399–412
40. **Taiz L** (1984) Plant cell expansion: regulation of cell wall mechanical properties. *Annu Rev Plant Physiol* **35**: 585–657
41. **Tazawa M, Kamiya N** (1965) Water relations of *Characean* internodal cell. Annual Report of Biological Workshop, Vol 13, Faculty of Science, University of Osaka, Osaka, Japan, pp 123–157
42. **Yamamoto R, Shinozaki K, Masuda Y** (1970) Stress-relaxation properties of plant cell walls with special reference to auxin action. *Plant Cell Physiol* **11**: 947–956
43. **Zimmermann U, Steudle E** (1975) The hydraulic conductivity and volumetric elastic modulus of cells and isolated cell walls of *Nitella* and *Chara* spp.: pressure and volume effects. *Aust J Plant Physiol* **2**: 1–12